

# RSC Advances



This is an *Accepted Manuscript*, which has been through the Royal Society of Chemistry peer review process and has been accepted for publication.

*Accepted Manuscripts* are published online shortly after acceptance, before technical editing, formatting and proof reading. Using this free service, authors can make their results available to the community, in citable form, before we publish the edited article. This *Accepted Manuscript* will be replaced by the edited, formatted and paginated article as soon as this is available.

You can find more information about *Accepted Manuscripts* in the [Information for Authors](#).

Please note that technical editing may introduce minor changes to the text and/or graphics, which may alter content. The journal's standard [Terms & Conditions](#) and the [Ethical guidelines](#) still apply. In no event shall the Royal Society of Chemistry be held responsible for any errors or omissions in this *Accepted Manuscript* or any consequences arising from the use of any information it contains.



Journal Name

ARTICLE

## Encapsulation tungstophosphoric acid into harmless MIL-101 (Fe) for effectively removing cationic dye from aqueous solution

Received 00th January 20xx,  
Accepted 00th January 20xx

DOI: 10.1039/x0xx00000x

www.rsc.org/

Ting-Ting Zhu, Zhi-Ming Zhang,\* Wei-Lin Chen, Zhu-Jun Liu and En-Bo Wang\*

A Keggin-type polyoxometalate  $H_3PW_{12}O_{40}$  ( $PW_{12}$ ) was firstly incorporated into the harmless porous metal organic framework MIL-101(Fe) resulting in POM@MOF composite material (denoted as  $PW_{12}$ @MIL-101). The material was synthesized by a one-pot solvothermal reaction of  $H_3PW_{12}O_{40}$ ,  $FeCl_3 \cdot 6H_2O$  and terephthalic acid ( $H_2bdc$ ). The composite was characterized by FTIR, XRD, thermogravimetric analyses (TGA), inductively coupled plasma (ICP) spectrometry, SEM, EDS,  $^{31}P$  NMR and nitrogen adsorption-desorption isotherms. These results demonstrated the successful insertion of  $H_3PW_{12}O_{40}$  within the cavities of MIL-101(Fe). The adsorption rate of the isolated MIL-101 was up to 30.7%, 28.3% for cationic dyes methylene blue (MB) and rhodamine B (RhB), and 82% for anionic dye methyl orange (MO) within 30 min. However, dye adsorption capacity of MIL-101 has greatly changed by introducing highly electronegative polyoxoanions to the cages of MIL-101. The adsorption rate of  $PW_{12}$ @MIL-101 composite was able to reach 99%, 96% for cationic dyes MB and RhB, and 16% for anionic dye MO in the initial 5 min. Surprisingly, the composite not only exhibited a large-scale adsorption capacity of 473.7 mg/g for MB, but also could quickly remove 97.3% MB from the dye solution with 1PPM (1mg/L). Furthermore, this material could be easily desorbed for reuse, and the structure of the composite was intact during the adsorption experiment. Thus, it is a promising and environmental friendly adsorbent for removing cationic organic pollutants in dye-wastewater.

### 1. Introduction

It is well known that organic dyes as an indispensable industrial production raw material is extensively used for cotton, linen, silk, textile, leather, printing paper industry and so on.<sup>1</sup> However, in recent years, with the rapid development of economy and industry, a large amount of dye-wastewater was directly discharged without reasonably processing, generating a tremendous threat to aqueous environment and human health on account of its toxicity and even carcinogenicity.<sup>2</sup> Therefore, it is urgent to find an effective approach to deal with organic dyes of the dye-wastewater before discharging it into the environment. So far, there are a variety of techniques which have been reported on the efficient elimination of hazardous and toxic organic dyes from aqueous solutions, such as membrane filtration,<sup>3</sup> coagulation,<sup>4</sup> photocatalysis,<sup>5</sup> advanced oxidation<sup>6</sup> and adsorption.<sup>7</sup> In the existing methods, adsorption is considered as a promising technology with high efficiency and low consumption to reduce the harmful pollutant contents of the contaminated water. To the best of our knowledge, activated carbons,<sup>8</sup>

zeolites,<sup>9</sup> polymeric materials<sup>10</sup> and graphene oxide<sup>11</sup> are common adsorbents in the treatment of dye-wastewater, whereas some of them are only effective for wastewater including low concentrations of dye and they are generally poor at selectively removing the targeted organic dye wastes. Hence, in this regard, it is extremely imperative to find a desirable adsorption material, which not only is capable of reducing the organic dyes in dye-wastewater with high efficiency and low loss, but also can achieve selective separation and recovery of raw materials.

Polyoxometalates (POMs), as an outstanding class of anionic metal oxide clusters, have attracted intensive attention due to their earth-abundant source, rich topology and versatility, controllable shape and size, oxo-enriched surfaces, highly electronegative etc,<sup>12</sup> which have various applications in many fields, such as catalysis,<sup>13</sup> optics,<sup>14</sup> magnetism,<sup>15</sup> biological medicine,<sup>16</sup> dye adsorption.<sup>17</sup> As a result, POMs are the potential and suitable adsorbent for selectively capturing cationic dyes as their strong attraction to cationic dyes. However, there are still obvious disadvantages for the POMs as adsorbents, such as (1) their relatively small surface area which seriously obstructs the accessibility to the active sites; (2) their excellent solubility in aqueous solution determines that they can not be reused and recycled in the process of wastewater treatment. Therefore, plenty of remarkable work has been done to encapsulate POMs into porous solid matrixes, such as activated carbon<sup>18</sup> and silica<sup>19</sup> for creating composite materials. Unfortunately, these methods sometimes lead to low POM

<sup>a</sup> Key Laboratory of Polyoxometalate Science of Ministry of Education, Department of Chemistry, Northeast Normal University, Changchun 130024 (P. R. China).  
E-mail: zhangzm178@nenu.edu.cn, wangeb889@nenu.edu.cn.

Electronic Supplementary Information (ESI) available: XRD results, TGA-DSC curves,  $^{31}P$  NMR, chemical structures of different dyes, the UV-Vis absorption spectra, EDS, ICP results and  $N_2$  adsorption-desorption results see DOI: 10.1039/x0xx00000x.

loading, it is thus of vital significance to search for an applicable solid matrix to immobilize POMs, which might greatly improve their adsorption ability for target dyes.

Currently, metal-organic frameworks (MOFs), as a relatively new class of porous materials<sup>20</sup> have attracted growing attention because of their crystalline nature, tunable structures and potential applications in the fields of gas storage and separation,<sup>21</sup> luminescence,<sup>22</sup> catalysis,<sup>23</sup> chemical sensing<sup>24</sup> and pollutant removal in water body<sup>25</sup> etc. Especially, the intrinsic superior porosity and incredibly large BET surface area of MOFs, have made them become a promising solid matrix for supporting POMs. In 2005, Férey et al. reported the incorporation of lacunary polytungstate [K<sub>7</sub>PW<sub>11</sub>O<sub>39</sub>] in the cages of MIL-101 (Cr) that firstly seized our attention.<sup>26</sup> In the recent two decades, there are a number of innovative and excellent POM @ MOF composites have emerged and been used in organic reaction,<sup>27,31</sup> electrocatalytic reaction,<sup>28</sup> photocatalytic reaction<sup>29</sup> and dye adsorption<sup>17a,17b,17d</sup>. [PW<sub>11</sub>CoO<sub>39</sub>]<sup>5-</sup>, [PW<sub>11</sub>TiO<sub>40</sub>]<sup>5-</sup>, [PW<sub>4</sub>O<sub>24</sub>]<sup>3-</sup> and [PW<sub>12</sub>O<sub>40</sub>]<sup>3-</sup>@MIL-101(Cr) composites were designed and synthesized, which were used as efficient catalysts in heterogeneous selective oxidation, alkene epoxidation, alcoholysis of styrene oxide and hydrolysis and esterification.<sup>27a,27b,27c,27d</sup> Then, the transition-metal substituted-POMs [PMo<sub>10</sub>V<sub>2</sub>O<sub>40</sub>]<sup>5-</sup> and [SiW<sub>11</sub>Fe<sup>III</sup>(H<sub>2</sub>O)<sub>39</sub>]<sup>5-</sup>,<sup>28a,28b</sup> the sandwich-type POMs Tb(PW<sub>11</sub>)<sub>2</sub> and Co<sub>4</sub>(PW<sub>9</sub>)<sub>2</sub> were all introduced into the MIL-101 (Cr) system.<sup>27e,27f,29</sup> Further, the HKUST MOF was used as the platform to encapsulate the POM anions, resulting in several remarkable and important crystalline compounds [H<sub>n</sub>XM<sub>12</sub>O<sub>40</sub>]@MOFs (X = Si, Ge, P, As; M= W, Mo) and [CuPW<sub>11</sub>O<sub>39</sub>]@HKUST by a simple one-step hydrothermal reaction.<sup>30</sup> Moreover, [PW<sub>12</sub>O<sub>40</sub>]<sup>3-</sup> was incorporated into MIL-100(Fe) by a simple low-temperature HF-free reaction.<sup>31</sup> So far, several typical POM@MOF composites have been used in dye adsorption. Wang's group synthesized three new compounds H<sub>3</sub>PW<sub>12</sub>O<sub>40</sub>, H<sub>4</sub>SiW<sub>12</sub>O<sub>40</sub> and H<sub>3</sub>PMo<sub>12</sub>O<sub>40</sub>@ZIF-8 by one-pot mechanochemical synthesis. These composites showed high uptake capacity for methylene blue.<sup>17b</sup> Yang et al prepared a new selective adsorbent H<sub>6</sub>P<sub>2</sub>W<sub>18</sub>O<sub>62</sub>/MOF-5, which exhibited a higher adsorption rate and selective adsorption ability for the cationic dyes than isolated MOF-5 framework.<sup>17d</sup> Our group synthesized a series of POM@MOF composite materials POM@MIL-101(Cr) (POM=K<sub>4</sub>PW<sub>11</sub>VO<sub>40</sub>, H<sub>3</sub>PW<sub>12</sub>O<sub>40</sub>, K<sub>4</sub>SiW<sub>12</sub>O<sub>40</sub>).<sup>17a</sup> These materials show excellent adsorption properties for the cationic dye. As mentioned above, it could find that MIL-101(Cr) is widely investigated in various reactions to incorporate the POM anions. Nevertheless, no effort has been dedicated to prepare POM@MIL-101(Fe) composite, although the Fe-based MOFs are much more harmless than that of the Cr-containing MOFs. In this regard, iron is a non-toxic and low-cost material, whereas chromium is a common poisonous element. Additionally, Cr<sup>3+</sup> in water body can be adsorbed on solid substances and present in sediments, which may cause severe chromium pollution.<sup>25f,32</sup> Thus, we choose MIL-101(Fe) as the platform to encapsulate POMs rather than MIL-101(Cr) that can completely avoid the possibility of chromium pollution.

In this study, a Keggin-type polyoxoanion [PW<sub>12</sub>O<sub>40</sub>]<sup>3-</sup> was firstly encapsulated into an eco-friendly framework MIL-101(Fe) generating a PW<sub>12</sub>@MIL-101 composite material by a simple one-pot reaction. For one thing, H<sub>3</sub>PW<sub>12</sub>O<sub>40</sub> with highly electronegative, hydrophilic and structural stability that could be utilized as a potential adsorbent for removal of the cationic dyes in dye-wastewater. For another, MIL-101(Fe) possessed of outstanding porosity and extremely large surface area, and it is insoluble in water, which is an appropriate solid matrix to encapsulate POMs. The combination of polyoxoanions and MIL-101(Fe) could improve the surface area and avoid the dissolution of POMs. The composite exhibited superior adsorption rate and selective adsorption ability for the cationic dyes. Remarkably, this material exhibited a large-scale adsorption capacity of 473.7mg/g for MB, which is much higher than that of the activated carbon.<sup>8</sup> Hence, it is a promising and environmental friendly adsorbent for removing and separating organic pollutants in dye-wastewater.

## 2. Results and discussion

### 2.1 Characterization of the composite

The FTIR spectra of H<sub>3</sub>PW<sub>12</sub>O<sub>40</sub>, MIL-101 and PW<sub>12</sub>@MIL-101 were performed on an Alpha Centauri FT/IR spectrophotometer using KBr pellets in the range of 4000–400 cm<sup>-1</sup>. As displayed in Fig. 1a, the absorption peaks of H<sub>3</sub>PW<sub>12</sub>O<sub>40</sub> at 1072, 972, 898 and 766 cm<sup>-1</sup> corresponding to the P-O<sub>a</sub>, W=O<sub>d</sub>, W-O<sub>b</sub>-W and W-O<sub>c</sub>-W band vibrations, the vibrational bands of MIL-101 located around 1601, 1383, 1042, 746 and 543 cm<sup>-1</sup> were all observed in the IR spectrum of PW<sub>12</sub>@MIL-101, which demonstrates the presence of PW<sub>12</sub>O<sub>40</sub> and MIL-101 in the POM@MIL-101 composite.

The XRD patterns of the MIL-101 and PW<sub>12</sub>@MIL-101 composite are shown in Fig. 1b. The peak positions of the as-synthesized MIL-101 matched well with the simulated pattern that based on the data of single-crystal structure. This revealed that the MIL-101 framework was successfully synthesized. From the Fig. 1b, we can discover that the representative patterns of MIL-101 still exist in the XRD pattern of PW<sub>12</sub>@MIL-101 composite. Besides, after the introduction of polyoxoanions into the cavity of MIL-101, the diffraction peaks at 2θ = 3.26, 6.88 and 7.28° slightly moved to the higher angle compared with the initial MIL-101. The deviation of XRD patterns were likely to the strong interaction between the polyoxoanions and the MIL-101 surface. Therefore, we can conclude that the framework of the MOF is stable during the process of encapsulating PW<sub>12</sub> into the cages of MIL-101. Moreover, the detailed XRD patterns of the composites PW<sub>12</sub>@MIL-101 with different loading of H<sub>3</sub>PW<sub>12</sub>O<sub>40</sub> can be seen in Fig. S1.

The thermogravimetric analyses (TGA) of MIL-101 and PW<sub>12</sub>@MIL-101 samples were carried out on a Perkin-Elmer TGA7 instrument in flowing N<sub>2</sub> with a heating rate of 10°C/min. As shown in Fig. 1c, the framework of MIL-101 and PW<sub>12</sub>@MIL-101 separately begins to collapse at 351°C and 364°C, revealing similar thermal stability. While the weightloss of PW<sub>12</sub>@MIL-101 is much lower than that of the isolated MIL-101 as the combination of the Keggin-type polyoxoanion into the MIL-101 framework. Besides, we tested the TGA-DSC curves of the pristine MIL-101, PW<sub>12</sub>@MIL-101, physical mixture of bulk PW<sub>12</sub> and MIL-101. The results indicated

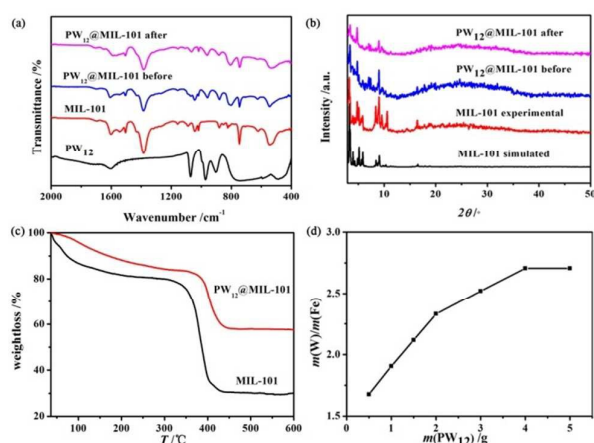


**Fig. 1** (a) IR spectra of  $PW_{12}$ , MIL-101 and  $PW_{12}@MIL-101$  before adsorption experiment and  $PW_{12}@MIL-101$  desorbed after adsorption experiment; (b) XRD patterns of MIL-101 and  $PW_{12}@MIL-101$ : the simulated XRD pattern of MIL-101, experimental XRD pattern of MIL-101 and  $PW_{12}@MIL-101$  before and after adsorption; (c) TGA of MIL-101 and  $PW_{12}@MIL-101$  under  $N_2$  atmosphere; (d) ICP analysis of the composite  $PW_{12}@MIL-101$  with different dosage of the POMs.

that the pristine MIL-101 and  $PW_{12}@MIL-101$  exhibited identical thermal stability (Fig. S2a, S2b). Whereas the physical mixture of bulk POM and MIL-101 displayed multi-step weight change compared with  $PW_{12}@MIL-101$  composite (Fig. S2b, S2c), which could also show  $PW_{12}$  is within the MIL-101. Thereby, the results of TG curves confirmed the successful immobilization  $PW_{12}$  to the MIL-101.

In order to further prove the existence of POMs in solid MOF matrix, elemental analysis for W and Fe were recorded on a Leaman inductively coupled plasma (ICP) spectrometer. In this work, we obtained a series of composites  $PW_{12}@MIL-101$  with different loading of POMs by a one-pot reaction. In Fig. 1d, it evinces that the loading amount of POMs reaches maximum when 4.0 g  $PW_{12}$  was employed in the synthesis of the composite material. Moreover, once the amount of  $PW_{12}$  was more than 4.0 g, the mass ratio of W and Fe in the composite almost remained unchanged with increasing the dosage of the POMs. The ICP results of  $PW_{12}@MIL-101$  composites were displayed in Table S1, including W (wt%), W/Fe (wt/wt),  $PW_{12}$  (wt%),  $PW_{12}$  ( $\mu\text{mol/g}$ ) and  $n(PW_{12})/n(MIL-101)$ . In the dye adsorption experiment, we used the  $PW_{12}\text{-}5\text{g}@MIL-101$  composite as adsorbent. The detailed ICP results of  $PW_{12}\text{-}5\text{g}@MIL-101$  were as follows. Elemental analysis showed that the W content in  $PW_{12}\text{-}5\text{g}@MIL-101$  was 30.56% and W/Fe (wt/wt) was 2.706. According to the elemental analysis results and molecular weight of  $H_3PW_{12}O_{40}\cdot nH_2O$  (2988 g/mol), the loading amount (wt%) of  $PW_{12}$  in  $PW_{12}@MIL-101$  was estimated to be 41.35%. Moreover, the content of hydrated  $PW_{12}$  was calculated based on the formula,  $PW_{12}$  ( $\mu\text{mol/g}$ ) =  $1 \times 10^6$  (W content in the hybrid material, %)/(2916  $\times$  W content in  $H_3PW_{12}O_{40}\cdot nH_2O$ ).<sup>27c</sup> The calculation results indicated that  $PW_{12}$  content in  $PW_{12}\text{-}5\text{g}@MIL-101$  material was 138.53  $\mu\text{mol/g}$ . Furthermore, the  $PW_{12}$  loading was 0.2061 for per MIL-101 (calculated based on the ratio of  $W_{12}/Fe_3$ , Table S1).

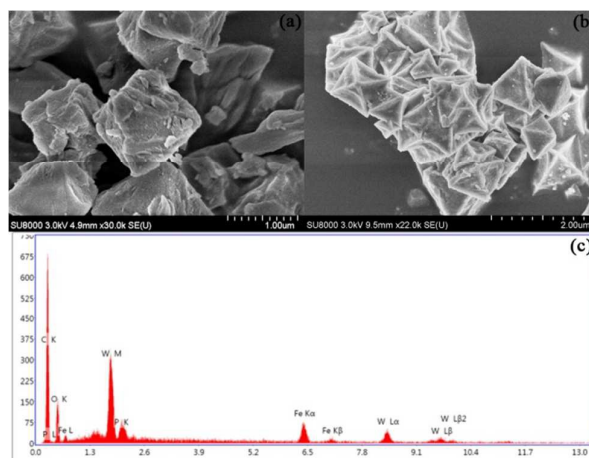


**Fig. 2** (a), (b) The SEM images of MIL-101 and  $PW_{12}@MIL-101$ . (c) The EDS of  $PW_{12}@MIL-101$ .

As revealed in Fig. 2a and 2b, the SEM images of MIL-101 and  $PW_{12}@MIL-101$  display similar polyhedral morphologies that are in good agreement with the reported one.<sup>34a</sup> From the Fig. 2a and 2b, we can easily find that the morphology of the  $PW_{12}@MIL-101$  maintain nearly unaffected after encapsulation of the  $PW_{12}$  into MIL-101. Additionally, the results also testify that the framework of MIL-101 does not degrade or collapse after the incorporation of  $[PW_{12}O_{40}]^{3-}$ . Furthermore, the EDS of  $PW_{12}@MIL-101$  composite material was tested, which showed the typical peaks of Fe, C, O, P, W in the  $PW_{12}@MIL-101$ . What's more, the EDS results manifested that W/Fe (wt/wt) was 2.698 in  $PW_{12}\text{-}5\text{g}@MIL-101$  and the  $PW_{12}$  loading was 0.2061 for per MIL-101, which is consistent with the ICP results. It indicated that  $PW_{12}$  existed in the composite material.

The  $^{31}\text{P}$   $\{^1\text{H}\}$  CP MAS spectra were recorded on a Bruker AVANCE III 400 WB spectrometer equipped with a 4 mm standard bore CP MAS probe head whose X channel was tuned to 162 MHz for  $^{31}\text{P}$ , using a magnetic field of 9.39T at 297 K. The dried and finely powdered samples were packed in the  $ZrO_2$  rotor closed with Kel-F cap which were spun at 12 kHz rate. The experiments were conducted at a contact time of 2 ms. A total of 800 scans were recorded with 3 s recycle delay for each sample. All  $^{31}\text{P}$  CP MAS chemical shifts are referenced to the resonances of monoammonium phosphate ( $NH_4H_2PO_4$ ) standard ( $\delta=0.00$ ). The  $^{31}\text{P}$   $\{^1\text{H}\}$  CP MAS spectra revealed a single signal at  $-17.1\text{ppm}$  confirming that the integrity of the Keggin structure was retained within the pores of MIL-101 (Fig. S3). Compared with the isolated  $H_3PW_{12}O_{40}$ , the characteristic peak of  $^{31}\text{P}$  generated slight deviation, which may attributed to the magnetic interference of  $Fe^{3+}$ .

The pore volume and BET surface area of the isolated MIL-101 and  $PW_{12}@MIL-101$  were determined by  $N_2$  adsorption-desorption isotherms at 77K. As presented in Fig. 3, MIL-101 had a pore volume and a BET surface area of  $1.398\text{cm}^3/\text{g}$  and  $2789\text{m}^2/\text{g}$ ; however,  $PW_{12}@MIL-101$  gave the lower pore volume ( $0.39\text{cm}^3/\text{g}$ ) and BET surface area ( $686\text{m}^2/\text{g}$ ) compared with the MIL-101. In addition, the pore size of the MIL-101 and

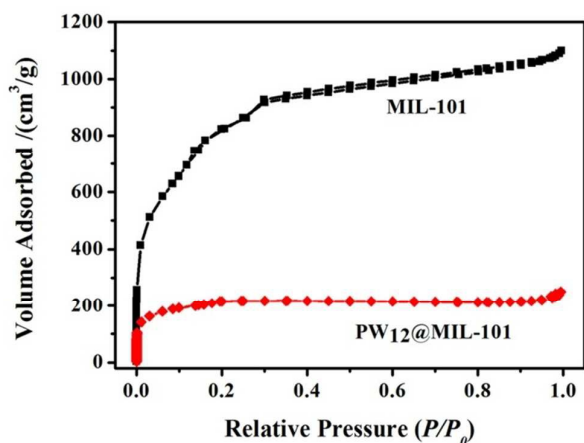


**Fig. 3** Nitrogen adsorption-desorption isotherms at 77K for MIL-101 (dark), PW<sub>12</sub>@MIL-101 (red).

PW<sub>12</sub>@MIL-101 were 4.12nm and 3.24nm that was calculated using BJH method (Table S2). Obviously, the PW<sub>12</sub>@MIL-101 showed smaller average pore size than that of MIL-101. The great difference between MIL-101 and PW<sub>12</sub>@MIL-101 was ascribed to the insertion of POMs into the pores of MIL-101 that can occupy part of the pore space. Furthermore, we carefully calculated the free space of MIL-101 that is occupied by the polyanions based on the ICP results, BET surface area and pore volume. The ICP results indicated that the loading amount (wt%) of PW<sub>12</sub> in PW<sub>12</sub>@MIL-101 was estimated to be 41.35%. Hence, the PW<sub>12</sub> occupied 950 m<sup>2</sup>/g and 0.578 cm<sup>3</sup>/g of the free space in MIL-101 according to BET surface area and pore volume. In a word, as mentioned above, the FTIR, XRD, TG, ICP, SEM, EDS, <sup>31</sup>P NMR and nitrogen adsorption-desorption isotherms collectively confirmed the successful incorporation of PW<sub>12</sub> anions and the MIL-101 framework.

## 2.2 Dye adsorption experiment

### 2.2.1 The effect of dye concentration

In this research, we choose a typical cationic dye MB as research object and systematically investigate the effect of dye concentration in the dye adsorption experiments. As exhibited in Fig. 4, the dye adsorption capacity of PW<sub>12</sub>@MIL-101 is largely influenced by the concentration of the dye solution. In the adsorption experiment, different concentrations of MB solution including 1, 5, 10, 20, 30, 40mg/L were prepared by diluting a solution of 100 mg/L MB, and 10mg PW<sub>12</sub>-5g@MIL-101 as adsorbent was employed for the removal of MB. In the Fig. 4, the UV-Vis spectroscopy results manifested that PW<sub>12</sub>@MIL-101 composite material displayed an excellent adsorption capacity to remove MB. Particularly, the adsorption rate of 100mL 5mg/L and 10mg/L MB solution fast reached to 99.5% and 99% respectively in the initial three minutes (Fig. 4a and 4b).

In addition, for the 40mg/L of MB (Fig. 4e), the adsorption rate of MB is still up to 96.2%. Interestingly, for the low concentration of the dye solution, this material can handle the level of PPM. The adsorption rate of MB solution with 1 PPM (1mg/L) is also able to reach 97.3% (Fig. 5). Hence, this material has potential

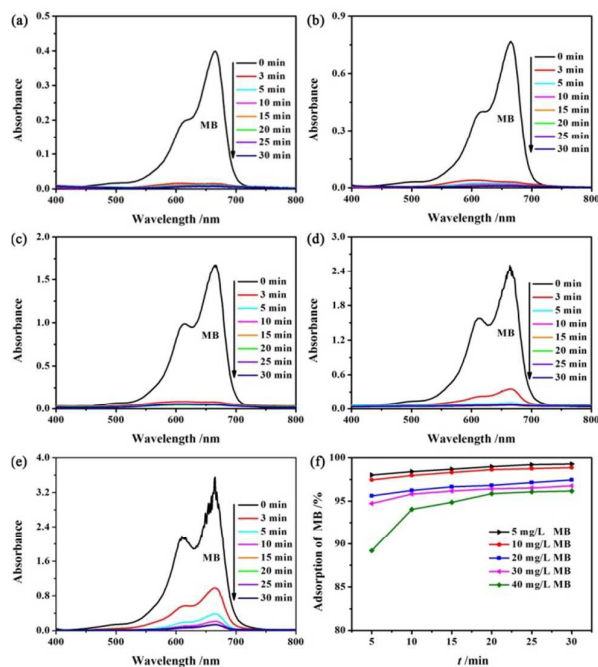


**Fig. 4** The UV-Vis spectrum of different concentrations of MB solution: (a) 5mg/L; (b) 10mg/L; (c) 20mg/L; (d) 30 mg/L; (e) 40 mg/L; (f) The adsorption rate of MB with diverse concentrations (mg/L): black: 5; red: 10; blue: 20; magenta: 30; olive: 40. Temperature: 293 K, adsorbent dose: 10 mg /100 mL.

applications in harnessing dye wastewater with either low concentration or high concentration.

### 2.2.2 The calculation of adsorption capacity and adsorption rate (Adsorption%)

The adsorption capacity  $Q_{eq}$ (mg/g) and adsorption rate (Adsorption%) were calculated according to the following equations:

$$Q_{eq} = \frac{(C_0 - C_{eq})V}{m} \quad (1)$$

$$\text{Adsorption}\% = \frac{(C_0 - C_t) \times 100\%}{C_0} = \frac{(A_0 - A_t) \times 100\%}{A_0} \quad (2)$$

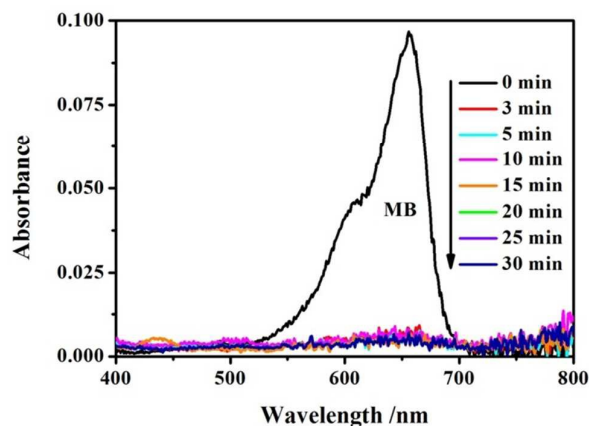


**Fig. 5** The UV-Vis spectrum of MB solution with 1PPM (1mg/L).

where  $C_0$ ,  $C_{eq}$  and  $C_t$  (mg/L) were the dye concentration of initial, equilibrium and at time  $t$ .  $Q_{eq}$  (mg/g) was the adsorption capacity of capacity of the dye, when it reached to adsorption equilibrium.  $A_0$  and  $A_t$  represented the absorbance of dye before and after adsorption.  $V$  (L) was the volume of the dye solution and  $m$  (g) was the dosage of the adsorbent.

The calibration curve of MB was obtained by analyzing data at 664nm with various concentrations of MB solution containing 5, 10, 20, 30, 40mg/L. After careful calculation, we can conclude that the adsorption capacity of MB is 473.7 mg/g when adding 20 mg  $PW_{12}$ -5g@MIL-101 in 100mL of 100 mg/L MB solution. Compared to the adsorbents that have been reported, such as activated carbons,<sup>8</sup> zeolites,<sup>9</sup> polymeric materials<sup>10</sup> and graphene oxide,<sup>11</sup>  $PW_{12}$ @MIL-101 exhibits much higher uptake capacity of MB (Table 1). Thus, this material is a promising adsorbent for the treatment of toxic organic pollutants in the dye-wastewater.

### 2.2.3 The comparison of adsorption capacity for different types of organic dyes in MIL-101 and $PW_{12}$ @MIL-101

To further demonstrate the role of anionic POMs in the composite material, the comparative experiment of MIL-101 and  $PW_{12}$ @MIL-101 was individually researched in removing the different types of organic dyes involving cationic dye MB, RhB and anionic dye MO. The detailed structures of dye molecules in the adsorption experiment were supplied in Fig. S5. Typically, 10mg adsorbent was added into 100ml 10mg/L dye solution under stirring, the concentration of the solution is measured in a given time.

As shown in Fig. 6a, 6c and 6e, the removal rate of the individual

**Table 1** Comparison of MB adsorption capacity in various adsorbents.

Adsorbents	Adsorption capacity (mg/g)	$C_{MB}$ (mg/L)	Ref.
Activated carbon	135	60	8, 17b
Zeolite	10.86	3.2	9
Polyaniline nanotubes	4.8	3.1	10
Graphene oxide	397	38.4	11
MOF@graphite oxide	18	36	25b
Zn-DDQ	135	500	25c
MOF-235	252	40	25a
MIL-100(Cr)	645.3	30	25d
MIL-100(Fe)	736.2	30	25d
Mesoporous MIL-101	22.5	30	25e
Nano- ZIF - 8	126	60	17b
Bulk ZIF-8	13.3	60	17b
$H_3PW_{12}O_{40}@Mn^{III}$ -porphyrin	10.5	10	17e
$H_3PW_{12}O_{40} \subset$ ZIF-8	810	200	17b
$PW_{11}V@MIL-101(Cr)$	371	100	17a
ErCu-POM (Er-3)	391.3	20	17c
$H_6P_2W_{18}O_{62}@MOF-5$	51.81	50	17d
$PW_{12}@MIL-101(Fe)$	473.7	100	This work

MIL-101 was separately up to 30.7%, 28.3% for cationic dyes MB, RhB, and 82% for anionic dye MO within 30 min. The reason for this phenomenon is that the framework of the MIL-101 is cationic.<sup>25a</sup> Thus, it represented superior adsorption capacity for anionic dye MO, whereas exhibited poor adsorption capacity for cationic dye MB and RhB (Fig. 6a, 6c and 6e). Especially, MIL-101 displayed worse adsorption capacity for RhB, which is because of its bigger volume than MB (Fig. 6a and 6c). Nevertheless, the adsorption capability of  $PW_{12}$ @MIL-101 was respectively able to reach 99%, 96% for cationic dyes MB and RhB, and 16% for anionic dye MO in the initial 5 min (Fig. 6b, 6d and 6f). Amazingly, after the introduction of polyoxoanions into the cavity of MIL-101, the adsorption capacity of POM@MIL-101 has changed a lot comparing with that of the isolated MIL-101 (Figure 6 and Figure 7). This is because that  $H_3PW_{12}O_{40}$  can be readily deprotonated and give polyanions. These anions can quickly and effectively adsorb MB and RhB cations, whereas strongly reject MO anions.<sup>17b</sup> In particular,  $PW_{12}$ @MIL-101 composite revealed a larger adsorption capacity for MB than RhB, which can attribute to its smaller volume (Fig. 6b and 6d). It is worth mentioning that a little uptake capacity of MO was observed for the POM@MIL-101, which was attributed to the surface adsorption between the dye molecules and cationic framework.

Further, the apparent difference between the MIL-101 and  $PW_{12}$ @MIL-101 was carefully detected and shown in Fig. 7. For  $PW_{12}$ @MIL-101, the concentration of MB and RhB decreases sharply in the first five minutes (Fig. 7a, 7b); whereas, the adsorption of MO is much slower and that the adsorption remains

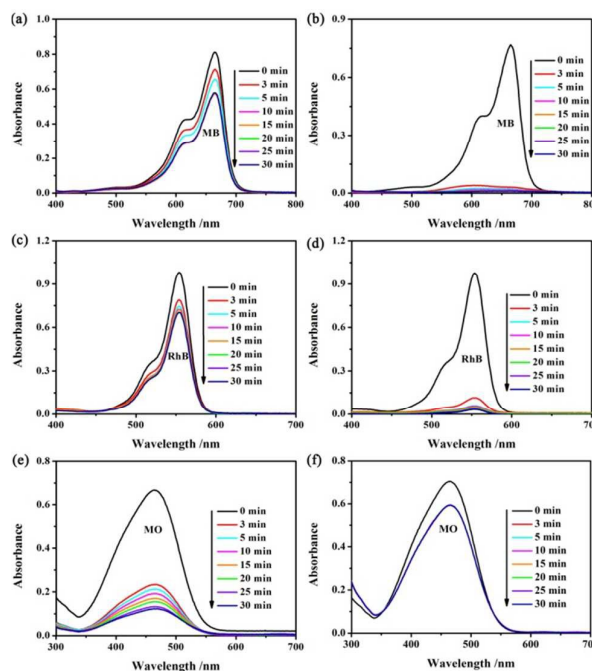


**Fig. 6** The temporal evolution of UV-Vis absorption spectra of MIL-101 and  $PW_{12}$ @MIL-101 toward different dyes. (a) MIL-101: 10mg/L MB; (b)  $PW_{12}$ @MIL-101: 10mg/L MB; (c) MIL-101: 10mg/L RhB; (d)  $PW_{12}$ @MIL-101: 10mg/L RhB; (e) MIL-101: 10mg/L MO; (f)  $PW_{12}$ @MIL-101: 10mg/L MO.

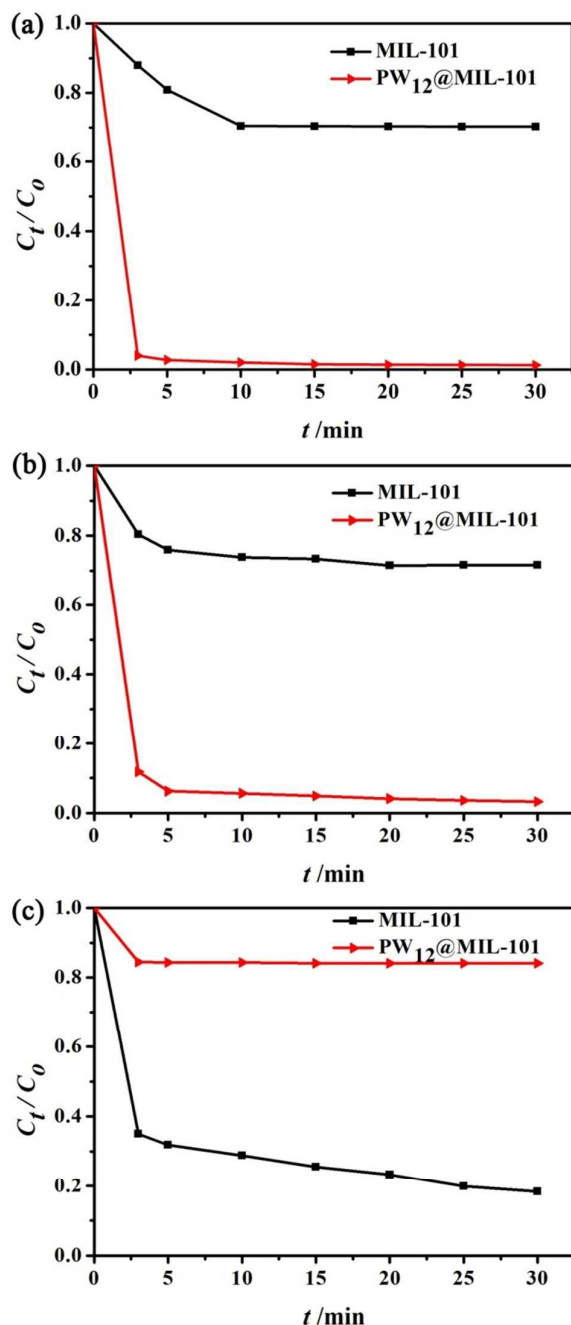


**Fig. 7** The concentration changes of different dye solution.  $C_0$  and  $C_t$  (mg/L) are the dye concentration of initial and at time  $t$ . (a) 10 mg/L MB; (b) 10 mg/L RhB; (c) 10 mg/L MO; black: MIL-101; red: PW<sub>12</sub>@MIL-101.

unchanged in several minutes. In contrast, the completely opposite results of MIL-101 are illustrated in Fig. 7c. It is a striking discovery that the existence of highly electronegative polyoxoanions greatly improved the adsorption ability of porous material MIL-101. It also indicates that the adsorption mechanism is mainly based on strong electrostatic interaction between the adsorbents and dye molecules. Furthermore, this

composite material also can't adsorb neutral dye in 10 mg/L SDI (Fig. S3), which further demonstrates that the adsorption mechanism is primarily dependent on electrostatic interaction. Accordingly, PW<sub>12</sub>@MIL-101 composite material is a superior adsorbent for cationic dyes in the dye-wastewater.

## 2.2.4 Selective adsorption ability of the composite material for the mixed organic dyes

Selective adsorption and separation of the specific dye is more attractive and challenging in the process of dye-wastewater treatment. In this study, in view of the large uptake capacity for MB, RhB in PW<sub>12</sub>@MIL-101, it can be anticipated that the composite material may also have an outstanding adsorption and separation behaviour in the treatment of a ternary mixture of MB, RhB and MO. To validate this point, further research is dedicated to investigate the separation of mixed dyes with different concentrations of MO, MB and RhB, including (1) 10, 5 and 5 mg/L; (2) 10, 10 and 10 mg/L; (3) 20, 10 and 10 mg/L of the above three dyes were respectively marked as mixed dye 1, 2 and 3.

As exhibited in Fig. 8a, 8c, 8e, the representative peaks of MB and RhB all disappeared quickly in mixed dye 1, 2 and 3, only the characteristic absorption peaks of MO left, suggesting that PW<sub>12</sub>@MIL-101 could selectively capture cationic dyes when utilized in the corresponding ternary mixture. The same

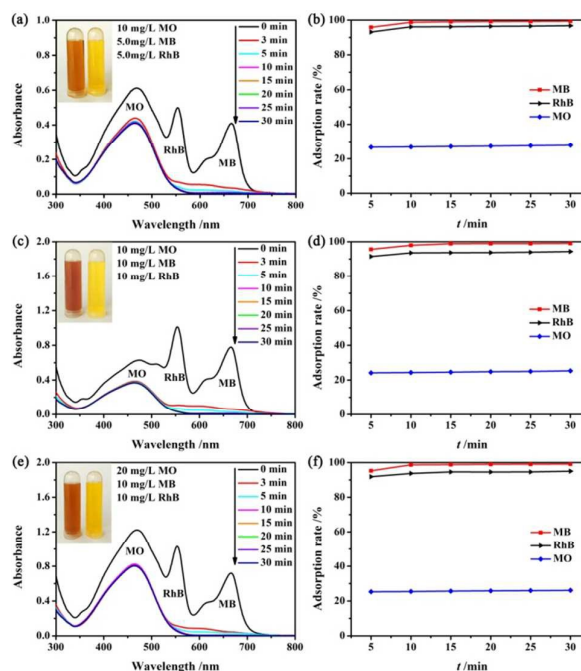


**Fig. 8** The UV-Vis absorption spectra and the dye adsorption rate of PW<sub>12</sub>@MIL-101 toward the mixed dyes solution with different concentration of MO, MB and RhB: (a) 10, 5 and 5 mg/L; (b) the adsorption rate of mixed dye 1; (c) 10, 10 and 10 mg/L; (d) the adsorption rate of mixed dye 2; (e) 20, 10 and 10 mg/L; (f) the adsorption rate of mixed dye 3. The colour change of the mixed dyes solution before (left) and after (right) adsorption process is inset in a, c, and e, respectively.

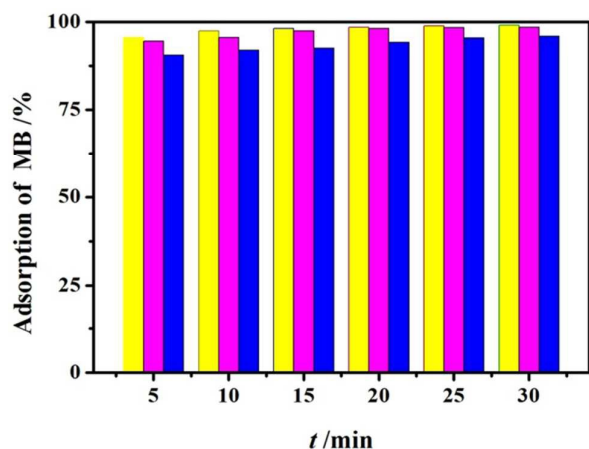


**Fig. 9** The reusability of PW<sub>12</sub>@MIL-101: yellow for the first cycle; magenta for the second cycle; blue for the third cycle

conclusion is displayed in the inset of Fig. 8, only the colour of MO can be seen in the final solution. Moreover, the adsorption rate of MB and RhB can reach around 99% and 96% as shown in Fig. 8b, 8d. Though MO molecules are small enough for ingress and egress of the windows of MIL-101, a little uptake capacity of MO was observed in Fig. 8f. It can be attributed to the negative charge of this dye molecule, which repels each other between MO and the POM caged in MIL-101. The slightly decreasing absorbance of MO is more likely to be adsorbed on the surface of adsorbents. The results further confirm that the electrostatic attraction is the key factor for the occurrence of adsorption. Thereby, PW<sub>12</sub>@MIL-101 composite material is an environmental friendly adsorbent for removing cationic organic pollutants after the encapsulation of POM anions. Further, the isolated MIL-101 is active for selective removal of the anionic dyes. So, the isolated and POM functionalized MIL-101 frameworks could be selected and used as the active adsorbent for removing different dyes.

### 2.2.5 The reusability and stability of the composite material

The stability and reusability of the adsorbents are an important standard for practical application. To verify whether the composite material is stable and recycled during the adsorption experiments, the cycle tests of PW<sub>12</sub>@MIL-101 on removing MB were explored. After each cycle, the adsorbent was completely separated by simple centrifugation because of its insoluble property in water. Subsequently, the fast release process of the adsorbed MB was achieved by thoroughly washing the adsorbent with a dilute solution of NaCl and DMF. Then, 10 mg desorbed adsorbent was added to 100 mL 10 mg/L MB solution under stirring. As described in Fig. 9, the composite material showed almost identically rapid adsorption of MB, and after two cycles, the regenerated adsorbent is still able to remove 96% MB from the solution. Thus, we may conclude that the composite material can be reusable during the adsorption experiment.

Moreover, the stability of this material is further discussed. As depicted in Fig. 1a, 1b, the FTIR spectrum and XRD pattern of the regenerated adsorbent are consistent with that of the as-synthesized composite. We can also observe representative

peaks of Fe, C, O, P and W from the EDS of the regenerated PW<sub>12</sub>@MIL-101 (Figure S4). Considering the above mentioned experiment results, we can conclude that the structure of the compound remain intact, which further confirms its excellent stability and recyclability.

## 3. Experimental

### 3.1 Materials and methods

All chemicals were commercially purchased and used without further purification. The H<sub>3</sub>PW<sub>12</sub>O<sub>40</sub><sup>33</sup> and MIL-101<sup>34</sup> were prepared according to literature procedures and characterized by using FTIR spectroscopy. X-ray powder diffraction data was collected on a Rigaku D/max-2550 diffractometer using Cu K $\alpha$  radiation. FTIR spectra was recorded on an Alpha Centauri FT/IR spectrophotometer with KBr pellets in the range of 4000-400 cm<sup>-1</sup> region at room temperature. The thermogravimetric analysis (TGA) was performed on a Perkin-Elmer TGA7 instrument in flowing N<sub>2</sub> with a heating rate of 10°C/min. Elemental analysis for W and Fe were measured by using a Leaman inductively coupled plasma (ICP) spectrometer. Scanning electron microscopy (SEM) images were obtained from FEI Quanta 200F microscope operated at an accelerating voltage of 20kV. Energy dispersive X-ray spectroscopy (EDS) was obtained from FEI Quanta 200F microscope. The <sup>31</sup>P {<sup>1</sup>H} CP MAS spectra were recorded on a Bruker AVANCE III 400 WB spectrometer. Nitrogen adsorption-desorption isotherms was tested by using a Micrometrics ASAP-2020 Mautomatic specific surface area and porous physical adsorption analyzer at 77K. UV-Vis absorption spectra were determined on a 756 CRT UV-Vis spectrophotometer.

### 3.2 Fabrication of MIL-101(Fe)

In a typical synthesis process, a mixture of 1.35g (4.9 mmol) of FeCl<sub>3</sub>·6H<sub>2</sub>O, 0.412g of H<sub>2</sub>bdc (2.48 mmol) and 30 mL DMF were completely dissolved under stirring. Subsequently, the resulting mixture was divided into 5 portions and transferred into a 13 mL Teflon-lined autoclave and heated at 110°C for 20 h. After cooling slowly to ambient temperature, the brown solid was collected and raw product was purified by a double treatment in ethanol at 60°C for 3 h. The product was dried at 60°C under vacuum.

### 3.3 Synthesis of composite PW<sub>12</sub>@MIL-101

The composite PW<sub>12</sub>@MIL-101 was synthesized by adding a moderate amount of H<sub>3</sub>PW<sub>12</sub>O<sub>40</sub> (0.5, 1.0, 1.5, 2.0, 3.0, 4.0, and 5.0 g) into the mixture of MOF precursors and stirred them for 30 min. The following experimental procedure is absolutely identical with the MIL-101(Fe).

### 3.4 Dye adsorption experiments

The dye adsorption experiments were performed in a 100 mL conical flask. Before adsorption experiments, the samples were activated by drying in a vacuum oven for 24 h at a

temperature of 120°C. In the adsorption experiments, the PW<sub>12</sub>@MIL-101 was added into dye solution with a definite concentration under stirring at room temperature. During a given time, the concentration of dye solution was obtained by measuring the absorbance on the UV/Vis spectrophotometer.

The used POM@MIL-101 was isolated from aqueous solution by centrifuging. Then, the adsorbed dye was removed by using a solution of NaCl and DMF under ultrasound at room temperature. The desorbed adsorbent powder was dried overnight at 120°C under vacuum.

#### 4. Conclusions

In summary, PW<sub>12</sub> anions were successfully introduced into the cages of MIL-101 by a simple one-pot reaction of H<sub>3</sub>PW<sub>12</sub>O<sub>40</sub>, FeCl<sub>3</sub>·6H<sub>2</sub>O, H<sub>2</sub>bdc and DMF. The adsorption efficiency of MIL-101 for cationic dyes MB and RhB in aqueous solution was observably improved after immobilizing high electronegativity and hydrophilic POMs into its cages. The adsorption rate of the dyes was extremely fast, which could also be seen in the low concentration dye solution of 1 PPM (1mg/L). Moreover, this material displayed a higher uptake capacity than that of the activated carbon.<sup>8</sup> Also, this composite was able to capture cationic dye molecules with unprecedented high selectivity. Therefore, the composite material not only exhibited high uptake capacity and fast absorption rate towards cationic dye, but also possessed the stability and reusability in the dye adsorption process. These remarkable results suggest that PW<sub>12</sub>@MIL-101 composite is a useful, economical and efficient adsorption and separation material, which can be further utilized in capture and separation of organic dyes in the contaminated water.

#### Acknowledgements

This work was financially supported by Science and Technology Development Project Foundation of Jilin Province (20150520001JH), Open Subject Foundation of Key Laboratory of Polyoxometalate Science of Ministry of Education, the Science and Technology Research Foundation of the Thirteenth Five Years of Jilin Educational Committee.

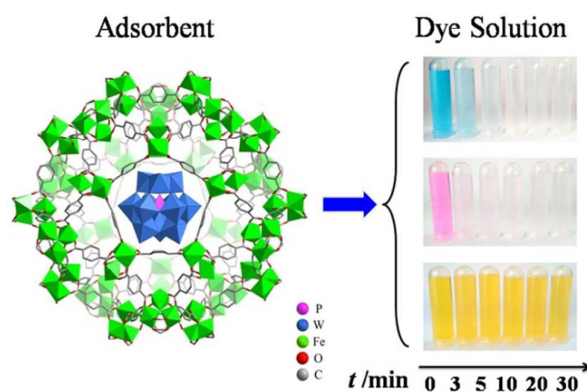
#### Notes and references

- 1 I. D. Rattee, *Chem. Soc. Rev.*, 1972, **1**, 145.
- 2 (a) W. Fan, W. Gao, C. Zhang, W. W. Tjiu, J. S. Pan and T. X. Liu, *J. Mater. Chem.*, 2012, **22**, 25108; (b) S. M. Wang, Y. Guan, L. P. Wang, W. Zhao, H. He, J. Xiao, S. G. Yang and C. Sun, *Appl. Catal. B: Environ.*, 2015, **168-169**, 448.
- 3 J. W. Lee, S. P. Choi, R. Thiruvengatachari, W. G. Shim and H. Moon, *Water Res.*, 2006, **40**, 435.
- 4 B. Y. Shi, G. H. Li, D. S. Wang, C. H. Feng and H. X. Tang, *J. Hazard. Mater.*, 2007, **143**, 567.
- 5 X. Y. Li, Y. H. Pi, Q. B. Xia, Z. Li, J. Xiao, *Appl. Catal. B: Environ.*, 2016, **191**, 192.
- 6 W. X. Chen, W. Y. Lu, Y. Y. Yao and M. H. Xu, *Environ. Sci. Technol.*, 2007, **41**, 6240.
- 7 (a) C. K. Karan and M. Bhattacharjee, *ACS Appl. Mater. Interfaces*, 2016, **8**, 5526. (b) H. M. Wang, C. Wang, S. Y. Tao,

- J. H. Qiu, Y. X. Yu and M. F. Gu, *ACS Sustainable Chem. Eng.*, 2016, **4**, 992. (c) H. X. Zeng and R. C. Tang, *RSC Adv.*, 2014, **4**, 38064.
- 8 The national standard of the People's Republic of China: wooden granular activated carbon for water purification. GB/T13803.2-1999.
- 9 C. D. Woolard, J. Strong, C. R. Erasmus, *Appl. Geochem.* 2002, **17**, 1159.
- 10 M. M. Ayad, A. A. El-Nasr, *J. Phys. Chem. C*, 2010, **114**, 14377.
- 11 F. Liu, S. Y. Chung, G. Oh and T. S. Seo, *ACS Appl. Mater. Interfaces*, 2012, **4**, 922.
- 12 (a) H. N. Miras, J. Yan, D. L. Long and L. Cronin, *Chem. Soc. Rev.*, 2012, **41**, 7403; (b) J. J. Gong, W. S. Zhang, Y. Liu, H. C. Zhang, H. L. Hu and Z. H. Kang, *Dalton Trans.*, 2012, **41**, 5468; (c) J. W. Zhang, J. H. Luo, P. M. Wang, B. Ding, Y. C. Huang, Z. L. Zhao, J. Zhang and Y. G. Wei, *Inorg. Chem.*, 2015, **54**, 2551; (d) C. H. Zhan, R. S. Winter, Q. Zheng, J. Yan, J. M. Carmeron, D. L. Long and L. Cronin, *Angew. Chem.*, 2015, **127**, 14516.
- 13 (a) S. S. Wang and G. Y. Yang, *Chem. Rev.*, 2015, **115**, 4893; (b) H. J. Yan, C. G. Tian, L. Sun, B. Wang, L. Wang, J. Yin, A. P. Wu and H. G. Fu, *Energy Environ. Sci.*, 2014, **7**, 1939; (c) X. B. Han, Y. G. Li, Z. M. Zhang, H. Q. Tan, Y. Lu and E. B. Wang, *J. Am. Chem. Soc.*, 2015, **137**, 5486.
- 14 J. S. Li, X. J. Sang, W. L. Chen, L. C. Zhang, Z. M. Zhu, Y. G. Li, Z. M. Su and E. B. Wang, *J. Mater. Chem. A*, 2015, **3**, 14573.
- 15 U. Kortz, A. Müller, J. V. Slagereen, J. Schnack, N. S. Dalal, M. Dressel, *Coord. Chem. Rev.*, 2009, **253**, 2315.
- 16 J. T. Rhule, C. L. Hill, D. A. Judd and R. F. Schinazi, *Chem. Rev.*, 1998, **98**, 327.
- 17 (a) A. X. Yan, S. Y. Y. G. Li, Z. M. Zhang, Y. Lu, W. L. Chen and E. B. Wang, *Chem. Eur. J.*, 2014, **20**, 6927; (b) R. Li, X. Q. Ren, J. S. Zhao, X. Feng, X. Jiang, X. X. Fan, Z. G. Lin, X. G. Li, C. G. Hu and B. Wang, *J. Mater. Chem. A*, 2014, **2**, 2168; (c) F. Y. Yi, W. Zhu, S. Dang, J. P. Li, D. Wu, Y. H. Li and Z. M. Sun, *Chem. Commun.*, 2015, **51**, 3336; (d) X. X. Liu, W. P. Gong, J. Luo, C. T. Zou, Y. Yang, S. J. Yang, *Appl. Surf. Sci.*, 2016, **362**, 517; (e) C. Zou, Z. J. Zhang, X. Xu, Q. H. Gong, J. Li and C. D. Wu, *J. Am. Chem. Soc.*, 2012, **134**, 87.
- 18 J. Alcañiz-Monge, G. Trautwein, S. Parres-Esclapez, J. A. Maciá-Agulló, *Micropor. Mesopor. Mat.*, 2008, **115**, 440.
- 19 Y. Chen, S. Zhao, Y. F. Song, *Appl. Catal. A: Gen.*, 2013, **466**, 307.
- 20 Q. L. Zhu and Q. Xu, *Chem. Soc. Rev.*, 2014, **43**, 5468.
- 21 E. D. Bloch, W. L. Queen, R. Krishna, J. M. Zadrozny, C. M. Brown, J. R. Long, *Science*, 2012, **335**, 1606.
- 22 Y. J. Cui, Y. F. Yue, G. D. Qian and B. L. Chen, *Chem. Rev.*, 2012, **112**, 1126.
- 23 Q. H. Yang, Q. Xu, S. H. Yu and H. L. Jiang, *Angew. Chem. Int. Ed.*, 2016, **55**, 3685.
- 24 S. Pramanik, C. Zheng, X. Zhang, T. J. Emge and J. Li, *J. Am. Chem. Soc.*, 2011, **133**, 4153.
- 25 (a) E. Haque, J. W. Jun, S. H. Jung, *J. Hazard. Mater.*, 2011, **185**, 507; (b) L. Li, X. L. Liu, H. Y. Geng, B. Hu, G. W. Song and Z. S. Xu; *J. Mater. Chem. A*, 2013, **1**, 10292; (c) Y. Zhu, Y. M. Wang, S. Y. Zhao, P. Liu, C. Wei, Y. L. Wu, C. K. Xia and J. M. Xie, *Inorg. Chem.*, 2014, **53**, 7692; (d) M. M. Tong, D. H. Liu, Q. Y. Yang, S. Devautour-Vinot, G. Maurin and C. L. Zhong, *J. Mater. Chem. A*, 2013, **1**, 8534; (e) X. X. Huang, L. G. Qiu, W. Zhang, Y. P. Yuan, X. Jiang, A. J. Xie, Y. H. Shen and J. F. Zhu, *CrystEngComm*, 2012, **14**, 1613; (f) S. R. Zhang, J. Li, D. Y. Du, J. S. Qin, S. L. Li, W. W. He, Z. M. Su and Y. Q. Lan, *J. Mater. Chem. A*, 2015, **3**, 23426.
- 26 G. Férey, C. Mellot-Draznieks, C. Serre, F. Millange, J. Dutour, S. Surblé, I. Margiolaki, *Science*, 2005, **309**, 2040.
- 27 (a) N. V. Maksimchuk, M. N. Timofeeva, M. S. Melgunov, A. N. Shmakov, Y. A. Chesalov, D. N. Dybtsev, V. P. Fedin and O. A. Kholdeeva, *J. Catal.*, 2008, **257**, 315; (b) N. V. Maksimchuk, K. A. Kovalenko, S. S. Arzumanov, Y. A. Chesalov, M. S.

- Melgunov, A. G. Stepanov, V. P. Fedin and O. A. Kholdeeva, *Inorg. Chem.*, 2010, **49**, 2920; (c) L. H. Wee, F. Bonino, C. Lamberti, S. Bordiga and J. A. Martens, *Green Chem.*, 2014, **16**, 1351; (d) Y. D. Zang, J. Shi, X. M. Zhao, L. C. Kong, F. M. Zhang, Y. J. Zhong, *Reac Kinet Mech Cat*, 2013, **109**, 77; (e) S. Ribeiro, C. M. Granadeiro, P. Silva, F. A. A. Paz, F. F. D. Biani, L. Cunha-Silva and S. S. Balula, *Catal. Sci. Technol.*, 2013, **3**, 2404; (f) S. S. Balula, C. M. Granadeiro, A. D. S. Barbosa, I. C. M. S. Santos and L. Cunha-Silva, *Catal. Today*, 2013, **210**, 142.
- 28 (a) D. M. Fernandes, A. D. S. Barbosa, J. Pires, S. S. Balula, L. Cunha-Silva and C. Freire, *ACS Appl. Mater. Interfaces*, 2013, **5**, 13382; (b) D. M. Fernandes, C. M. Granadeiro, P. M. P. D. Sousa, R. Grazina, J. J. G. Moura, P. Silva, F. A. A. Paz, L. Cunha-Silva, S. S. Balula and C. Freire, *ChemElectroChem*, 2014, **1**, 1293.
- 29 J. Y. Han, D. P. Wang, Y. H. Du, S. B. Xi, Z. Chen, S. M. Yin, T. H. Zhou, R. Xu, *Appl. Catal. A: Gen.*, 2016, **521**, 83.
- 30 (a) C. Y. Sun, S. X. Liu, D. D. Liang, K. Z. Shao, Y. H. Ren and Z. M. Su, *J. Am. Chem. Soc.*, 2009, **131**, 1883; (b) J. Song, Z. Luo, D. K. Britt, H. Furukawa, O. M. Yaghi, K. I. Hardcastle and C. L. Hill, *J. Am. Chem. Soc.*, 2011, **133**, 16839.
- 31 F. M. Zhang, Y. Jin, J. Shi, Y. J. Zhong, W. D. Zhu and M. S. El-Shall, *Chem Eng J*, 2015, **269**, 236.
- 32 T. A. Saleh, S. A. Haladu and S. A. Ali, *Chem. Eng. J.*, 2015, **269**, 9.
- 33 J. C. Bailar, H. S. Booth and G. M. Booth, *Inorg Synth*, 1939, **1**, 132.
- 34 (a) K. M. L. Taylor-Pashow, J. D. Rocca, Z. G. Xie, S. Tran and W. B. Lin, *J. Am. Chem. Soc.*, 2009, **131**, 14261; (b) N. V. Maksimchuk, K. A. Kovalenko, V. P. Fedin and O. A. Kholdeeva, *Chem. Commun.*, 2012, **48**, 6812.

## Graphical



$\text{H}_3\text{PW}_{12}\text{O}_{40}$  was firstly incorporated into the cages of harmless MIL-101(Fe). The composite material exhibited excellent adsorption performance for cationic dyes MB and RhB, which can be utilized in selective capture and separation of organic dyes in the contaminated water. Moreover, the adsorbent is reusable and stable, the removal of MB can also reach 96% after two cycles.